



Imagent

functional Near Infrared Imaging System (fNIRS) Brain Imaging using Infrared Photons

The Principle

It has been known for more than 100 years that specific types of neurological deficits are induced by lesions to particular areas of the brain. The observational data accumulated in this past century indicate that the brain can be viewed as a complex information-processing center comprising structures specialized for different types of functions. Different areas work together to produce complex behavior that may be disrupted if the communication between areas is severed. In the past 20 years, cognitive psychologists and neuroscientists have increasingly converged their mutual observations towards a comprehensive theory of brain/mind function, this new discipline being named "cognitive neuroscience."

Non-invasive functional brain imaging techniques are instrumental in advancing the discipline, as they allow the researcher to derive measures of physiological activity of the human brain. Functional information, versus structural, derives from the slow (> 100 ms) and fast (< 100 ms) optical signals observed during brain stimulation. Functional measurements have been reported on the motor cortex during motor stimulation; on the visual cortex during visual stimulation; on the frontal region during mental work; and on the monitoring of cerebral hemodynamics during sleep.

Brain imaging techniques can be broadly classified in two groups. One group includes the techniques that have a good spatial resolution (up to 1-2 millimeters) but a poor temporal resolution, such as functional Magnetic Resonance Imaging (fMRI) and Positron Emission Tomography (PET). The second group includes techniques featuring an excellent temporal resolution (of the order of milliseconds) but providing a limited spatial information. This group includes the Event Related Brain Potential (ERP) and the Magneto-encephalography (MEG).

The ISS Imagent provides a balance between temporal and spatial resolution for the study of superficially located areas of human brain. Imagent detects variations in the oxygenation levels of activated brain areas and provides a map of the areas where the changes occur. This new instrument's working principle is based on the use of near infrared light for probing the cortical surface. In fact, the penetration depth of light in tissues is quite significant in the wavelength range from 650 nm to 900 nm. The main absorbers in this spectral region are oxy and deoxy-hemoglobin. On a smaller scale, water, fat and cytochrome oxidase contribute to the partial absorption of the light. For typical head tissue (skin/scalp, skull and cortical layer), with an absorption coefficient of $\mu_a = 0.1 \text{ cm}^{-1}$ and a scattering coefficient $\mu_s' = 8 \text{ cm}^{-1}$, the maximum optical penetration can be estimated to be about 1.5 cm when a detector is placed at 4 cm from the source. The penetration depth can be increased by increasing the distance between the source and the detector, although, eventually, the signal-to-noise ratio of the measurement deteriorates.

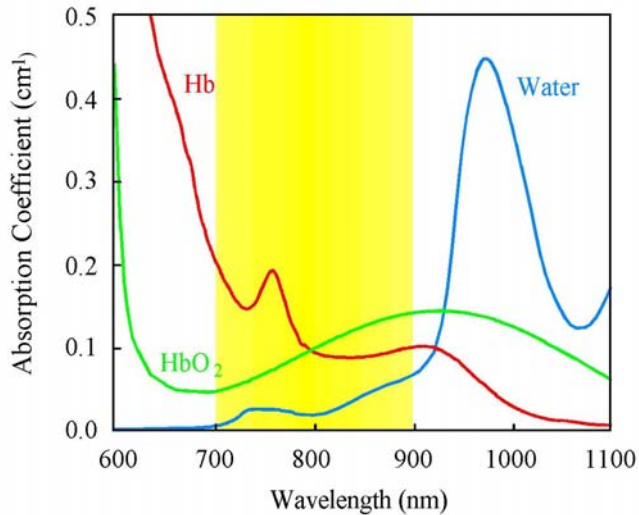


Figure 1. Main tissue absorbers in the region 600 1100 nm.

Imagent utilizes laser diodes emitting at two wavelengths, 690 nm and 830 nm, respectively and modulated at 240 MHz. The instrument is available in two versions: the ω -version features sixty four (64) emitters and eight light detectors while the δ -version features thirty two (32) sources and four detectors. Each light source is turned ON/OFF by the computer in a sequence determined by the operator to ensure that the signal emitted by each source is correctly identified by the detectors. Typically, the ON time for a light source is about 20 ms - although a longer or shorter time can be selected - and the entire cycle for eight light sources may take 160 ms. This is the measurement time for characterizing the hemodynamics changes occurring in a region.

For the detection of fast signals - signals related to neuronal activation - one wavelength only is typically utilized. In this mode of operation, it is feasible to have a readout time in less than 20 ms.

Three modes of operation are selectable through the software and reported in Table I and Table II for the δ -version and the ω -version, respectively. The instrument is versatile as it allows the researcher to utilize a smaller number of light sources and probe a region in a short time.

The light that traversed the tissue is collected by fiber bundles, which divert it to the light detectors. Three components of the detected signal are measured: the DC and AC component, as well as the phase of the photon density wave. The use of the AC and phase components, contrary to the DC component of the signal, assures that the room light does not interfere with the measurement. Additionally, modulated light penetrates the tissue at a deeper depth than non-modulated light. The light is delivered to the tissue by fiber optics, which are arranged in a geometrical pattern selected by the researcher. The sources are turned ON/OFF sequentially by the computer, thus allowing the probing of different regions in the area covered by the probe. The different source-detector distances allow the researcher to probe different depths in the same region, as well as an estimate of the scattering and absorption coefficient in the region.

Operation mode	No. of sources ON simultaneously	Typical cycle time * (ms)	Typical max cycle time EROS (ms)	No. of detectors	Description
Switch-8	4	160 or less	16 or less	4	Each of the 4 laser boards has one LD ON for 20 ms. The signal is collected simultaneously on 4 detector channels. Since 4 light sources are on simultaneously, they must be positioned far apart from one another.
Switch-16	2	320 or less	32 or less		Only 2 LDs are ON simultaneously. The signal is collected simultaneously on 4 detector channels. The probes can be positioned closer together as fewer light sources are on simultaneously.
Switch-32	1	320 or less	64 or less		In this mode of operation, the cycle time is long, but fewer light sources are on simultaneously so more positions can be probed closer together. In this mode, there is only one light source on at a time for 10 ms.
Table I. Mode of operation for Imagent δ -version (32 sources)					

* Typical for monitoring hemoglobin changes. Depending on the computer, experimental conditions, etc. both the typical times shown above can be faster.

Imagent includes a computer for instrument control and data reduction; a data acquisition card for Fast-Fourier-Transform acquisition of frequency domain data; and a complete ISS Boxy Software package for data collection (AC, DC and phase), data manipulation and storage, and real time graphing.

Operation mode	No. of sources ON simultaneously	Typical cycle time* (ms)	Typical max cycle time EROS (ms)	No. of detectors	Description
Switch-8	8	160 or less	16 or less	8	Each of the 4 laser boards has one LD ON for 20 ms. The signal is collected simultaneously on 8 detector channels. Since 4 light sources are on simultaneously, they must be positioned far apart from one another.
Switch-16	4	320 or less	32 or less		Only 2 LDs are ON simultaneously. The signal is collected simultaneously on 8 detector channels. The probes can be positioned closer together as fewer light sources are on simultaneously.
Switch-32	2	320 or less	64 or less		In this mode of operation, the cycle time is long, but fewer light sources are on simultaneously so more positions can be probed closer together. In this mode, there are only two light sources on at a time for 10 ms.
Table I. Mode of operation for Imagent ω -version (64 sources)					

Probe Patterns

While ISS is not currently supplying sensors for the Imagent, several probe patterns that are available with Imagent and have been used by our customers are shown below. Figure 2 shows a pattern using sixteen sources (eight emitting at 690 nm and the remaining eight emitting at 830 nm) arranged at eight locations around the four detectors.

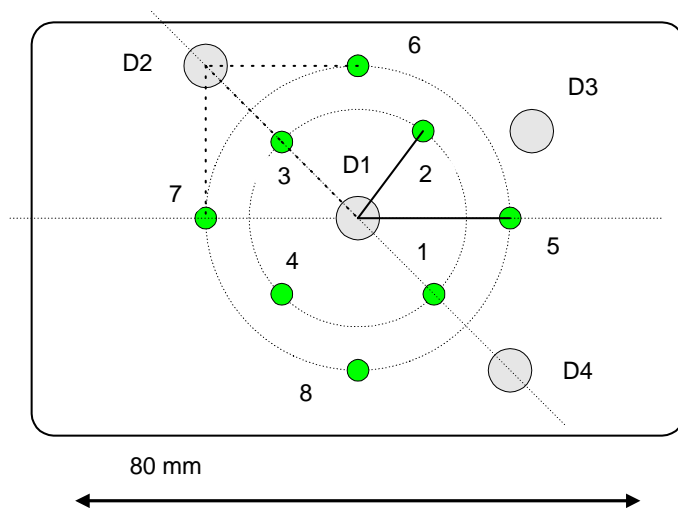


Figure 2. In this pattern, the eight sources emitting radiation at 690 nm are placed on two concentric circles of different diameters. The sources 1 to 4 on one circle and the sources 5 to 8 on a larger-diameter circle. While detector D1 is placed at the center of the circles, detectors D2-D4 are placed at different locations providing a variety of distances for the sources.

The signal from the sources located closer to the detectors probes the superficial layer, while the signal detected from the probes located at further distances from the detector probe a deeper region. In this way, it is possible to separate the contribution of the different layers to the signal. In this configuration, the entire readout of the region occurs in 160 ms. The additional sixteen sources can be arranged around this pattern to enlarge the region under examination.

Figure 3 displays schematically a second arrangement of sources and detectors using the Imagent d-version. The signal coming from crossed pairs as in the region delimited by a dashed line, allows for a better localization of the area.

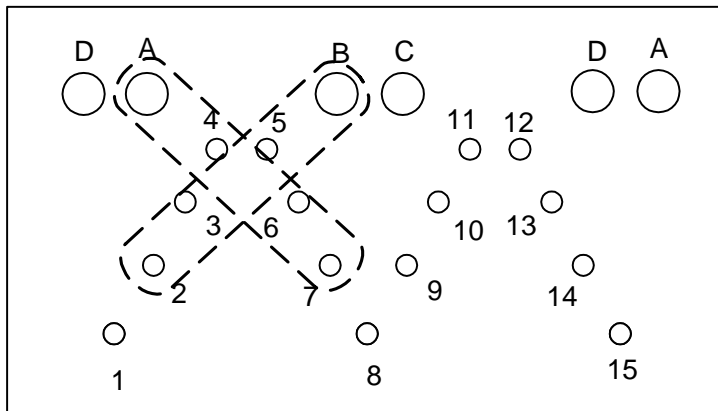


Figure 3. Schematic of the region of optical probe used for the measurements of hemodynamics fluctuations in the human brain. The dashed lines delimit a region using the crossed source-detector pattern for data acquisition.

Applications

The probe of Figure 3 was applied on the head of volunteers in the position indicated in Figure 4 (left side of the head in the motor cortex area). The subjects were asked to begin or stop performing a finger-motion (palm squeezing) exercise using the right hand. The squeezing rhythm (1.5 Hz) was maintained by means of a metronome. Exercise epochs typically had stimulation/relaxation periods of 20/20 s, 20/13 s and 17/10 s, and each consisted of 10 periods.

Figure 5 shows the hemodynamics fluctuations measured in source-detector pairs A7 and D15. In Fig. 5a one can see that during the stimulation, the oxy-hemoglobin concentration $[HbO_2]$ increases and the deoxy-hemoglobin concentration $[Hb]$ decreases, and during the relaxation there is a recovery toward the baseline level. This pattern of hemodynamic changes during the exercise is obviously different from the one observed at rest. Figure 5b displays the signal detected at location D15: at this location there is no significant difference between the fluctuation patterns at rest and during exercise (the full scale of Fig. 5a is 0.25, while the full scale of the plot of Fig. 5b is 0.15).

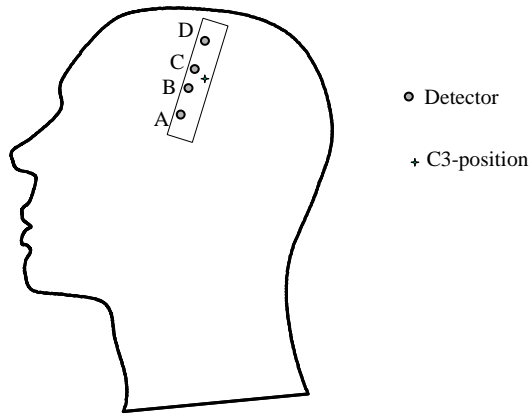


Figure 4. Position of the optical probe on the head

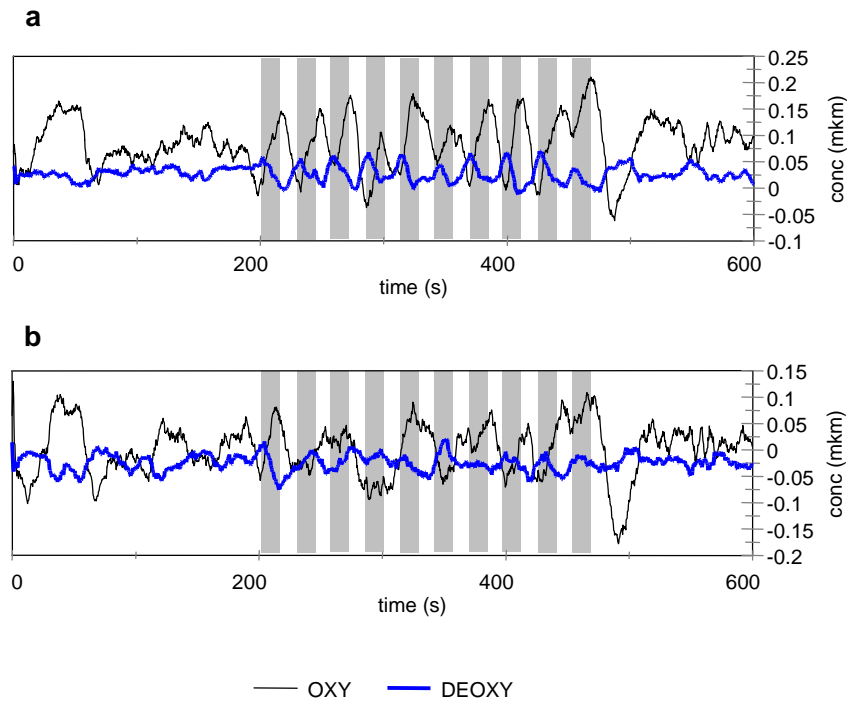


Figure 5. Hemodynamics fluctuation measured in source–detector pairs A7 (a) and D15 (b)

References

A. Brain Imaging

1. **S. Fantini, D. Hueber, M. A. Franceschini, E. Gratton, W. Rosenfeld, P. G. Stubblefield, and M. R. Stankovic;**
Non-invasive Optical Monitoring of the Newborn Piglet Brain Using Continuous-wave and Frequency-domain Spectroscopy;
Phys. Med. Biol., 44 (1999) 1543-1563.
2. **S. Fantini, M.A. Franceschini, E. Gratton, D. Hueber, W. Rosenfeld, D. Maulik, P. Stubblefield, and M.R. Stankovic;**
Non-invasive optical mapping of the piglet brain in real time;
Optics Express. 4(8), (1999) 308-314.).
3. **M.A. Franceschini, V. Toronov, M. Filiaci, E. Gratton and S. Fantini;**
On-line optical imaging of the human brain with 160-ms temporal resolution;
Optics Express 6, 49-57 (2000).
4. **D. M. Hueber, M A. Franceschini, H. Y. Ma, Q. Zhang, J. R. Ballesteros, S. Fantini, D. Wallace, V. Ntziachristos and B. Chance;**
Non-invasive and quantitative near-infrared hemoglobin spectrometry in the piglet brain during hypoxic stress, using a frequency-domain multi-distance instrument;
Submitted to Physics in Medicine and Biology, (June 2000).
5. **M.R. Stankovic, D. Maulik, W. Rosenfeld, P.G. Stubblefield, A.D. Kofinas, S. Drexler, R. Nair, M.A. Franceschini, D. Hueber, E. Gratton, and S. Fantini;**
Real-time optical imaging of experimental brain ischemia and hemorrhage in neonatal piglets;
J. of Perinatal Medicine. 27(4), (1999) 279-286.
6. **V. Toronov, A. Webb, J. H. Choi, M. Wolf, A. Michalos, E Gratton, and D. Hueber;**
Investigation of human brain hemodynamics by simultaneous near-infrared spectroscopy and functional magnetic resonance imaging,
Submitted to Proc. Natl. Acad. Sci., (July 2000).

B. Fast Signals (*EROS*: Event Related Optical Signal)

1. **Gratton G., M. Fabiani, D. Friedman, M. A. Franceschini, S. Fantini, P. M. Corballis, and E. Gratton;**
"Rapid Changes of Optical Parameters in the Human Brain During a Tapping Task",
J. Cognitive Neuroscience **7**, 446-456 (1995).
2. **Gratton G., P. M. Corballis, E. Cho, M. Fabiani, and D. C. Hood;**
"Shades of gray matter: non-invasive optical images of human brain responses during visual stimulation",
Psychophysiology **32**, 505-509 (1995).
3. **Gratton G. and M. Fabiani;**
"Dynamic brain imaging: Event-related optical signal (*EROS*) measures of the time course and localization of cognitive-related activity",
Psychonomic Bulletin & Review **5**, 535-563 (1998).
4. **Gratton G., M. Fabiani, M.R. Goodman-Wood, and M.C. DeSoto;**
"Memory-driven processing in human medial occipital cortex: An event-related optical signal (*EROS*) study",
Psychophysiology **35**, 348-351 (1998).
5. **Gratton G., A. Sarno, E. Maclin, P. M. Corballis, and M. Fabiani;**
Neuroimage **11**, 491-504 (2000).
6. **Rinne T., G. Gratton, M. Fabiani, N. Cowan, E. Maclin, A. Stinard, J. Sinkkonen, K. Alho, and Risto Näätänen;**
"Scalp-Recorded Optical Signals Make Sound Processing in the Auditory Cortex Visible",
NeuroImage **10**, 620-624 (1999).

For more information please call (217) 359-8681
or visit our website at www.iss.com



1602 Newton Drive
Champaign, Illinois 61822 USA
Telephone: (217) 359-8681
Telefax: (217) 359-7879
Email: iss@iss.com